Energy & Buildings 208 (2020) 109634

Contents lists available at ScienceDirect

Energy & Buildings

journal homepage: www.elsevier.com/locate/enbuild

Effect of climate conditions on the thermodynamic performance of a data center cooling system under water-side economization

Andrés J. Díaz[a,*], Rodrigo Cáceres[a], Rodrigo Torres[a], José M. Cardemil[b], Luis Silva-Llanca[c]

[a] Escuela de Ingeniería Industrial, Facultad de Ingeniería y Ciencias, Universidad Diego Portales, Av. Ejército 441, Santiago, Chile
[b] Departamento de Ingeniería Mecánica, Facultad de Ciencias Físicas y Matemáticas, Universidad de Chile, Av. Beauchef 851, Santiago, Chile
[c] Instituto de Investigación Multidisciplinario en Ciencia y Tecnología, Departamento de Ingeniería Mecánica, Facultad de Ingeniería, Universidad de La Serena, Benavente 980, La Serena, Chile

ARTICLE INFO

Article history:
Received 2 October 2018
Revised 7 October 2019
Accepted 24 November 2019
Available online 25 November 2019

Keywords:
Water-side economizer
Free-cooling
Water consumption
Data center

ABSTRACT

This paper evaluates the potential of water-side economizers in the refrigeration system of data centers under different climate conditions. Due to the wide range of conditions along the country (Desert, Mediterranean, Temperate rainy and Tundra climate), Chile is selected as case study. The number of hours per year in which economization is possible is estimated using the data base of 22 weather stations along the country. The refrigeration system is modeled in steady state through a set of thermodynamic equations simultaneously solved using the Engineering Equation Solver (EES). The system performance is evaluated by calculating the Coefficient of Performance (COP) and the Water to Energy Ratio (WER). The latter is a new metric proposed to compare the volume of water required by the system to save 1 MWh of cooling energy. The thermodynamic analysis shows that the chiller decreases its energy usage if water-side economizers are implemented in favorable climates such as cool-summer Mediterranean with winter rain (Csc), temperate rainy (Cfb) and tundra (ET) climates. Here, the use of economizers allows a monthly increase in the COP of 50 to 120% (compared to the conventional operation) and an annual average COP ranging from 7.8 to 9.7. These climates also offer an additional gain of lower water requirements, with annual WER values ranging from 11 to 17 m^3/MWh. Desert climates, on the other hand, prevent implementing economizers, offering the lowest annual average COP values (5.6–5.7). In climates in which the complete economization is impossible, the partial use of economizers allows a monthly increase in the COP of 10 to 45%. The costal influence decreases the system performance, reducing the COP and increasing the WER.

1. Introduction

The data center industry experienced a substantial growth during the last decade, leading to a significant increase in its energy demand [1]. Despite energy efficiency measures deployed, particularly in developed nations, the energy use remains in steady growth, showing no sign of deceleration for the upcoming years. For instance, data centers in the United States are expected to consume nearly 73 billion kWh in 2020, corresponding to a yearly increase rate of 4% between 2014 and 2020 [2].

Efficient thermal management improves the energy and environmental performance of data centers mainly for two reasons: (1) Approximately 40% of the energy consumed by legacy data centers corresponds to refrigeration (HVAC) [3]; and (2) for each kWh consumed, 1.8 liters of water are required by the refrigeration system [2]. Both cooling energy and water consumption are investigated in this paper, seeking to further the knowledge about the impact of energy efficiency techniques on the water demand of the system.

Water consumption in data centers has become an important issue to be considered for designing cooling systems. Algorithms have been proposed to optimize its use [4]; a metric has been defined to estimate the ratio of the total water consumption to the IT energy use, known as the Water Usage Effectiveness (WUE) [5]; a Water Footprint analysis has been proposed to evaluate the data center's facilities [6]; and new cooling systems have been evaluated in terms of their capacity to reduce the water consumption [7].

Regarding cooling energy use, several operational methods, design strategies and technology solutions exist for improving how heat is managed in data centers, such as the implementation of: hot or cold aisle containment, localized cooling, solar or geothermal cooling, waste heat recovery and economizers. Some authors

* Corresponding author.
E-mail address: andres.diaz@udp.cl (A.J. Díaz).

https://doi.org/10.1016/j.enbuild.2019.109634
0378-7788/

Nomenclature

COP	Coefficient of Performance
$\dot{C}$	heat capacity rate, kW/K
f	frequency
h	enthalpy, kJ/kg
$load$	chiller's cooling load
$\dot{m}$	mass flow, kg/s
P	pressure, kPa
$\dot{Q}$	heat transfer rate, kW
RH	Relative Humidity
T	temperature, °C
$\dot{\forall}$	flow rate, m^3/s
$\dot{W}$	power, kW
WER	Water to Energy Ratio, m^3/MWh

Subscripts

air	air
amb	ambient
annual	annual
c	conventional
cf	complete free-cooling
c + m	controllers and monitoring system
Chiller	relative to the chiller
CRAH	relative to the CRAH units
CWP	Condensed Water Pump
eva	chiller's evaporator
fan	relative to the fan
m	monthly
mains	mains
max	maximum
min	minimum
n	nominal
pf	partial free-cooling
pumps	relative to the pumps
PP	Primary Pump
rack	rack
ref	referential
room	white room
SP	Secondary Pump
system	relative to the system
tower	relative to the cooling tower

Greek symbols

α	phase angle
ε	effectiveness
ω	humidity ratio

have also used the concept of Exergy Destruction minimization to quantify energy savings in data centers [8–12].

Capozzoli and Primiceri [13] summarized the advantages and disadvantages in the current state of the existing technologies, emphasizing the energy saving potential of utilizing economizers. According to Ni and Bai [14] (in a summary of the energy performance of 100 data center cooling systems in 2017), more than half of the data centers they evaluated operate in inefficient conditions, where the highest potential for improving the energy conservation in this industry is represented by the implementation of economizer cycles.

Economizer systems use the data center surrounding environmental conditions in favor of the heat transfer, providing what is often called "free-cooling" [15–29]. Two types of economizers are found in data centers: air-side and water-side economizers. The former uses the filtered cool outside air to remove the heat from the data center room; the latter uses the facility's cooling tower to directly cool the chilled water. Choosing between the most suitable option depends on the components employed for removing the heat [30] and electricity prices [31]. Even when some authors claim that air economizers are more effective than water economizers [32–34], their use could result unattractive in locations with low electricity prices or high humidification demand. Nonetheless, both cases reduce the use of compressors, thus the system achieves significant energy savings, decreasing its Power Usage Effectiveness (PUE).

Deymi-Dashtebayaz et al. [23] notably combined air-side and water-side economizers, along with an air source heat pump for waste heat recovery. They reported energy savings of up to 250 MWh per year – improving the PUE by 16% – and a yearly CO_2 emission reduction of 267 tons. Zhang et al. [27] estimated a potential water-based free-cooling operation during 17% of the year in a region located in northern China, with an extra 32% when operated in conjunction with traditional electrical cooling. They claimed an average PUE of 1.35.

According to estimates from 2008 [35], the effective use of economizers in representative cities within the United States reduced the Data Centers energy demand by about 20 to 25%. However, in hot and humid areas, both air-side and water-side economizer systems remain unviable [36,37]. The benefits associated with the use of economizers, and the overall thermal performance of data centers, strongly depend on the local weather conditions [19,30,35,38–43], rendering geographic location as a crucial aspect in data center design.

The present work studies the effect of climate conditions on both cooling energy and water consumption levels in data centers by either evaluating the possibility of completely or partially reducing the chiller energy use. Water-side economizers are employed since they have been recognized not only as a technique to reduce the cooling energy demand, but also as complement for other novel thermal management techniques such as: aisle containment [44], Multi-stage Outdoor Air (MOA) [45], heat pipe loops [46], thermosyphons [28], liquid desiccant or evaporative cooling [45], and temperature adaptive control strategies [47].

To the best of our knowledge, water-side economization studies mostly focus on energy and economic savings, essentially neglecting the water consumption aspect. We intend to emphasize water savings, especially for geographic regions where the resource is scarce, such as a large portion of the Chilean territory.

The specific goals of this paper are:

- Elucidating the relationship between the increase in energy efficiency and water consumption, since the literature lacks a detailed approach for correlating water consumption with the reduction in the cooling energy use levels
- Estimating the number of water-side free-cooling hours under different climate conditions
- Estimating the effect of climate condition on the data center's thermodynamic performance, since cooling energy use has been shown to be highly dependent on its geographic location [48].

2. System description and modeling

2.1. Refrigeration system

This paper evaluates the thermodynamic performance of the refrigeration system shown in Fig. 1, which is used to provide cold air (0.3 m^3/s at $T_1 = 20^oC$, $P_1 = 1$ bar and 50% RH) to 42 racks that dissipate $\dot{Q}_{rack} = 15kW$ each. The refrigeration system has been modified from [9] and includes a water-side cooling economizer, a counter flow wet cooling tower and a condensed water loop. Table 1 summarizes the operating conditions of each of

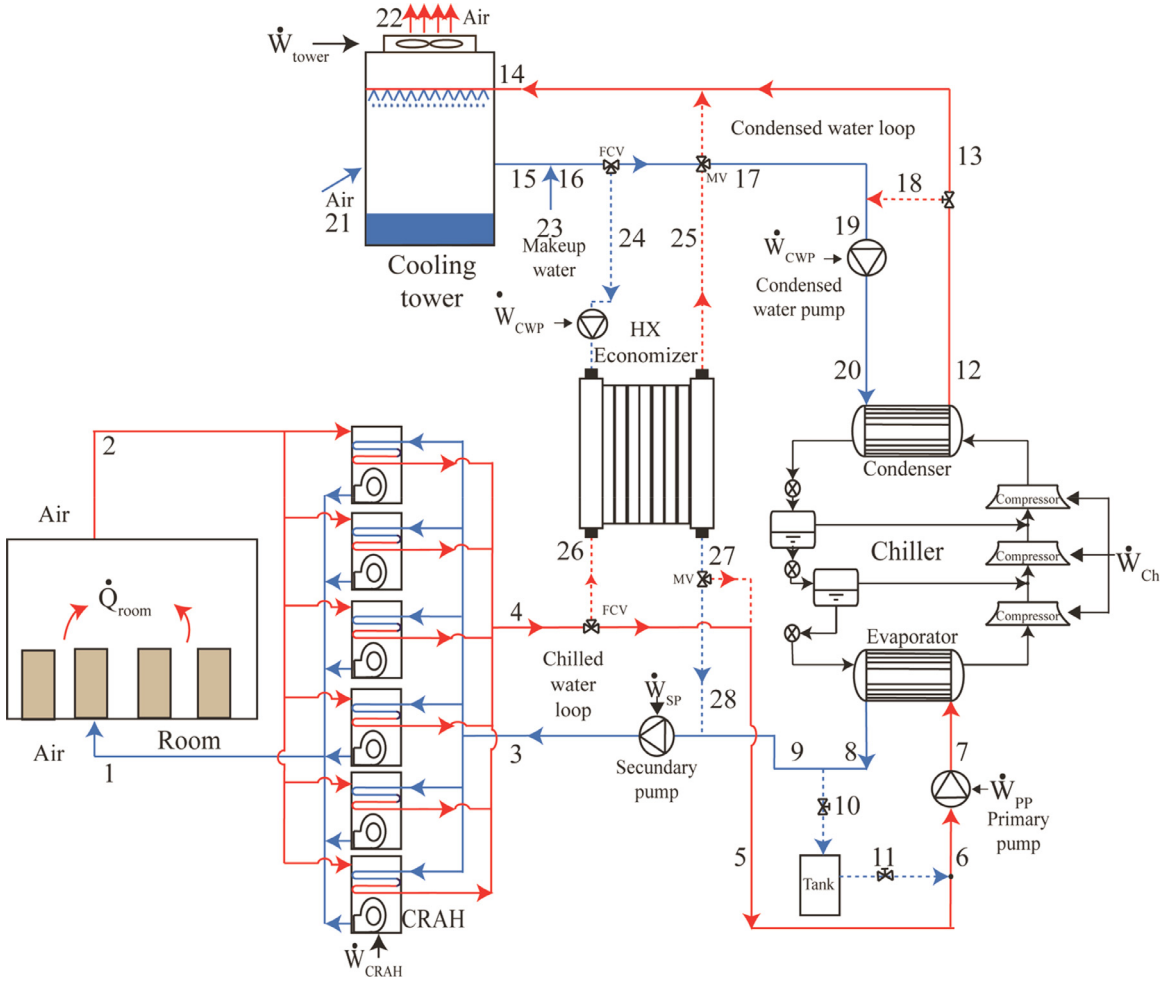

Fig. 1. Refrigeration system schematic.

the system components, selected according to the manufacturer's recommendation.

In the proposed refrigeration system, air exits the cooling tower as saturated (100% relative humidity). To prevent freezing, a lower limit of 3^oC is established for the water leaving the tower.

A condensed water loop is used to guarantee that a temperature of at least $T_{19} = T_{20} = 20^oC$ enters the condenser. Here, a Condensed Water Pump (CWP) is used to rise the pressure from $P_{19} = 1$bar to $P_{20} = 3$bar, as suggested by the chiller's manufacturer.

Table 1
Refrigeration system specifications.

Component	Parameter	Value
Room	Number of racks	42
	Heat transfer rate per rack	15 kW
	Air flow per rack	0.3 m^3/s
CRAH Uniflair, Leonardo Evolution	Heat flow dissipation capacity	118.6 kW
TDCV 4300	Controllers and monitoring system power consumption	3.26 kW
	Fan nominal power consumption	5.44 kW
	Maximum air flow rate	8.33 m^3/s
	Maximum water flow rate	0.00473 m^3/s
Chiller Trane CVHE	Water flow rate through the evaporator	0.035 m^3/s
	Water flow rate through the condenser	0.056 m^3/s
	Cooling capacity	1055.06 kW
Plate heat exchanger Armstrong SX29	Effectiveness	90%
Counter flow wet cooling tower	Fan nominal power consumption	10 kW
Marley NCF8402	Maximum air flow rate	78.29 m^3/s
Primary pump Grundfos NK	Isentropic efficiency	80.4%
100–250/266, 50 Hz	Pressure drop	0.9 bar
Secondary pump Grundfos NK	Isentropic efficiency	80.2%
100–315/334, 50 Hz	Pressure drop	2 bar
Condensed water pump Grundfos NK	Isentropic efficiency	80.11%
100–315/334, 50 Hz	Pressure drop	2 bar

Fig. 2. Map of the selected meteorological stations within the Chilean territory.

The performance of the refrigeration system is evaluated under different weather conditions using the 22 weather stations shown in Fig. 2 and Table 2. Environmental properties are extracted from the data base of the Chilean Meteorological Direction from 2011 to 2015, which provides the minimum, maximum and daily average of pressure, dry-bulb temperature and Relative Humidity (RH). Details of each of the selected climate conditions, categorized according to the Köppen climate classification, is provided in Table 3.

Thus, depending on the environmental conditions, the economizer seeks to replace a chiller that provides cold water at $P_8 = 1\text{bar}$ and $T_8 = 6^oC$(state at which the manufacturer characterizes the chiller power consumption). The same pressure and temperature are assumed for states 9, 10 and 11 (water loop). In this manner, the complete free-cooling mode is active if the economizer is able to provide water at $T_{27} = 6^oC$. The partial free-cooling mode is active when the economizer provides water between 6 and 12^oC. This upper limit considers the recommended water temperature variation within the selected CRAH units ($T_4 - T_3 = 6^oC$), where$T_3 = T_8$. Consequently, if the economizer provides water at a temperature $\geq 12^oC$, the system operates in conventional mode (without the economizer).

2.2. Thermodynamic modeling

A thermodynamic analysis is conducted to evaluate the cooling energy and water consumption. The working fluids are air and water, which flow under steady state conditions and with negligible pressure drops (see Fig. 1). The environmental properties are assumed to vary hourly, for which the inbuilt functions of the Engineering Equation Solver (EES) [49] software are used to estimate the required thermos-physical properties. This software is widely used by the scientific community dealing with macroscopic thermodynamic related simulations, for either power cycles [50] or for cooling applications [9]. The software allows the computation of algebraic equations governing heat transfer phenomena through its built-in numeric solver, and also easily communicates with a thermos-physical properties database based on REFPROP-NIST [51]. Since energy and mass balances are performed in each device of the refrigeration system, the EES software identifies groups of equations to be solved iteratively by means of the

Table 2
Location of the selected meteorological stations.

Station	Climate main classification		Köppen classification	City	Latitude	Longitude
1	Arid	Desert climate	BWh	Arica	−18.49111	−70.30139
2			BWh	Iquique	−20.53972	−70.17861
3			BWk	Calama	−22.49530	−69.90440
4			BWk	Antofagasta	−23.68083	−70.44110
5	Temperate	Mediterranean climate	Csb	Santiago	−33.44500	−70.68280
6			Csb	Curicó	−34.96640	−71.21670
7			Csb	Chillán	−36.58720	−72.04000
8			Csb	Los Angeles	−37.40280	−72.42250
9			Csb (i)	Rodelillo	−33.06833	−71.55750
10			Csb (i)	Santo Domingo	−33.65500	−71.61420
11			Csb (i)	Concepción	−36.77920	−73.06220
12			Csc	Punta Arenas	−53.15270	−70.92630
13			Csc	Puerto Natales	−51.66720	−72.52880
14			Csc	Porvenir	−53.25361	−70.32611
15		Temperate rainy	Cfb	Alto Palena	−43.61170	−71.80530
16			Cfb	Puerto Aysén	−45.39940	−72.67720
17			Cfb	Coyhaique	−45.59390	−72.10860
18			Cfb (i)	Puerto Montt	−41.43500	−73.09750
19			Cfb (s)	Valdivia	−39.65060	−73.08080
20			Cfb (s)	Temuco	−38.77000	−72.63190
21			Cfb (s)	Osorno	−40.60500	−73.06080
22	Polar	Tundra	ET	Puerto Williams	−54.93170	−67.61560

Table 3
Description of Köppen classification.

Köppen classification	Description
BWh	Hot desert
BWk	Cold desert
Csb	Warm-summer Mediterranean with winter rain
Csb (i)	Warm-summer Mediterranean with winter rain and coastal influence
Csc	Cool-summer Mediterranean with winter rain
Cfb	Temperate rainy
Cfb (i)	Temperate rainy with coastal influence
Cfb (s)	Temperate rainy with short summer drought periods
ET	Tundra

Newton-Raphson and the Tarjan blocking algorithm. Here, the stop criterion considers 250 iterations with a residual less than 1×10^{-6}, in which each iteration considers a change in variables less than 1×10^{-9}.

2.2.1. Estimation of cooling energy use

To estimate the cooling energy use, the Coefficient of Performance (COP) is calculated to relate the overall heat dissipated by the racks to the total power consumed by entire the refrigeration system, as follows

$$COP_{system} = \frac{\dot{Q}_{room}}{\dot{W}_{system}} = \frac{n_{racks}\dot{Q}_{rack}}{\dot{W}_{CRAH} + \dot{W}_{chiller} + \dot{W}_{tower} + \dot{W}_{pumps}} \quad (1)$$

Here, the CRAH power consumption is calculated considering the power associated with the fan and controllers and monitoring system (see Table 1)

$$\dot{W}_{CRAH} = \dot{W}_{c+m} + \dot{W}_{fan,CRAH} \quad (2)$$

The fan power of the CRAH units is calculated as function of the air flow rate as suggested by the fan law

$$\dot{W}_{fan,CRAH} = \dot{W}_{fan,CRAH,n}\left(\frac{\dot{\forall}_{air,CRAH}}{\dot{\forall}_{air,CRAH,\max}}\right)^3 \quad (3)$$

According to the manufacturer, at $T_8 = 6^oC$, the selected chiller requires a nominal power of 21.2 kW under a *load* of 13%, whereas for a *load* of 100% it requires 180.9 kW. The *load* is defined as the ratio of the heat flow dissipated by the evaporator ($\dot{Q}_{eva}$) to the chiller cooling capacity (1055.06 kW). As suggested by Meakins [52], the chiller power demand can be correlated to a third grade polynomial function of the *load* as follows

$$\dot{W}_{chiller} = 18.4257 + 31.6728(load) + 0.822349(load)^2 + 131.048(load)^3 \quad [\text{kW}] \quad (4)$$

The constants of Eq. (4) offer an R^2 value of 99.91%. Eq. (4) requires solving an energy balance first to calculate $\dot{Q}_{eva}$.

The cooling tower power consumption ($\dot{W}_{tower}$) depends only on its fan power consumption, which is calculated similar to Eq. (3). In accordance to the manufacturer's recommendations, the ratio of the water to air flow within the tower is assumed to be 1.2. Thus,

$$\dot{W}_{tower} = \dot{W}_{tower,n}\left(\frac{\dot{m}_{14}}{1.2\rho_{21}\dot{\forall}_{air,tower,\max}}\right)^3 \quad (5)$$

The total power consumption of all pumps ($\dot{W}_{pumps}$) is obtained considering each of the isentropic efficiencies, recommended pressure drops and flow rates of water (obtained through energy balances).

2.2.2. Makeup water consumption

Since a water supply system must be employed to compensate the water evaporation within the cooling tower, this paper evaluates the impact of reducing the cooling energy demand on the water consumed by the system. The goal is to identify the effect of each of the selected climate conditions in terms of their use of natural resources. The Water to Energy Ratio (WER) is proposed as a new metric to compare the water required by the cooling tower (when economization is possible) with the energy savings. Thus,

$$\text{WER} \equiv \frac{\text{Water consumption}}{\text{Energy savings}}\left[\frac{\text{m}^3}{\text{MWh}}\right] \quad (6)$$

The water consumption can be estimated through the mass flow rate of water leaving the cooling tower due to evaporation [53], which is a function of the difference in humidity between the air entering and exiting the cooling tower.

The estimation of the energy savings requires assuming that the system always operates in conventional mode. Thus, the maximum energy demand can be calculated. If the economizer is able to provide cold water, allowing to reduce the chiller load, then the system will consume less energy than the conventional mode, and energy savings will exist. The energy savings represent the difference between the maximum energy use and the energy used by the system when either partial or complete free-cooling is available.

Therefore, for each hour of operation, the WER is calculated as follows

$$\text{WER} = \begin{cases} \dfrac{\dot{m}_{23}}{\dot{W}_{system,c} - \dot{W}_{system,cf}} & \text{if complete free} - \text{cooling is active} \\ \dfrac{\dot{m}_{23}}{\dot{W}_{system,c} - \dot{W}_{system,pf}} & \text{if partial free} - \text{cooling is active} \end{cases} \quad (7)$$

where

$$\dot{m}_{23} = \dot{m}_{21}(\omega_{22} - \omega_{21}) \quad (8)$$

Both ω_{21} and ω_{22} are obtained using the inbuilt functions of EES. State 21 is given by the environmental data, whereas state 22 assumes atmospheric pressure and saturated air. In addition, T_{22} is obtained through an energy balance in the cooling tower.

The temperature of the makeup water (T_{23}) is estimated at each location as function of ambient, surface and ground temperature, according to the model proposed by Burch and Christensen [54]. Thus,

$$T_{23} = \left[T_{mains,annual} - \Delta T_{mains}\sin\left(f_{annual}t - \alpha_{amb} - \alpha_{mains}\right) - 32\right]\frac{5}{9} \quad (9)$$

Here, $T_{mains,\ annual}$ represents the annual average temperature of the water supplied by the distribution network, given by

$$T_{mains,annual} = T_{amb,annual} + \Delta T \quad (10)$$

where $T_{amb,\ annual}$ is the annual average ambient temperature at each location, which assumes a temperature shift of $\Delta T = 3.33^oC$. In Eq. (9), ΔT_{mains} is proportional to the ambient temperature and the pipes depth, which is estimated as follows

$$\Delta T_{mains} = 0.9R(T_{max,m} - T_{min,m}) \quad (11)$$

Table 4
Monthly average temperature and relative humidity at the selected stations.

	January		February		March		April		May		June	
Station	T, °C	RH	T, °C	RH	T, °C	RH	T, °C	RH	T, °C	RH	T, °C	RH
1	22.4	0.61	23.2	0.61	22.4	0.63	20.7	0.65	19.3	0.67	17.9	0.65
2	21.6	0.61	22.4	0.60	21.0	0.64	19.3	0.65	18.1	0.66	17.0	0.67
3	22.3	0.33	23.0	0.42	22.2	0.39	20.5	0.30	19.1	0.23	17.7	0.19
4	22.3	0.70	23.0	0.71	22.2	0.73	20.5	0.73	19.1	0.73	17.7	0.73
5	21.8	0.49	21.3	0.49	19.4	0.54	15.5	0.63	12.6	0.70	9.8	0.74
6	21.7	0.56	20.9	0.60	19.3	0.61	15.4	0.65	12.7	0.71	10.0	0.71
7	20.5	0.61	19.3	0.64	13.6	0.69	10.4	0.76	10.5	0.86	8.5	0.90
8	20.7	0.51	19.3	0.54	16.7	0.63	12.8	0.70	10.2	0.71	8.6	0.73
9	17.2	0.76	17.4	0.74	16.6	0.75	14.6	0.77	13.2	0.81	11.6	0.77
10	16.7	0.77	16.1	0.78	13.4	0.81	12.4	0.80	12.0	0.83	10.9	0.81
11	17.5	0.74	16.7	0.76	15.5	0.78	13.4	0.84	11.9	0.88	10.6	0.85
12	11.3	0.62	10.7	0.65	9.6	0.72	6.8	0.77	4.5	0.80	2.6	0.82
13	11.9	0.61	11.6	0.64	10.1	0.66	5.5	0.73	2.9	0.83	2.5	0.77
14	11.5	0.67	10.8	0.70	9.8	0.74	7.4	0.78	4.4	0.82	2.6	0.83
15	13.5	0.55	12.0	0.58	10.1	0.64	8.0	0.76	6.1	0.81	4.5	0.80
16	12.0	0.72	11.6	0.74	7.3	0.80	6.2	0.85	6.0	0.87	4.3	0.85
17	15.4	0.59	14.1	0.65	11.6	0.67	9.2	0.73	6.7	0.81	4.6	0.80
18	15.3	0.78	14.3	0.82	13.0	0.83	11.1	0.88	9.9	0.90	7.5	0.90
19	17.6	0.68	16.3	0.74	13.9	0.80	11.8	0.89	10.6	0.92	8.1	0.92
20	17.6	0.55	16.6	0.57	14.6	0.62	11.9	0.67	10.4	0.70	8.3	0.67
21	16.7	0.61	15.5	0.66	13.4	0.70	11.1	0.79	9.9	0.63	7.2	0.64
22	10.0	0.69	9.2	0.72	8.6	0.74	6.3	0.77	4.0	0.80	2.3	0.81
	July		August		September		October		November		December	
Station	T, °C	RH	T, °C	RH	T, °C	RH	T, °C	RH	T, °C	RH	T, °C	RH
1	16.5	0.70	16.5	0.71	17.2	0.71	18.3	0.70	19.9	0.65	21.6	0.63
2	15.3	0.68	15.5	0.68	16.4	0.68	17.3	0.66	18.8	0.63	20.6	0.62
3	16.4	0.18	16.3	0.16	17.1	0.15	18.1	0.15	19.8	0.16	21.4	0.22
4	16.4	0.74	16.3	0.74	17.1	0.73	18.1	0.71	19.8	0.69	21.4	0.69
5	9.2	0.74	11.2	0.72	13.4	0.66	15.5	0.58	18.1	0.49	20.5	0.47
6	9.2	0.72	10.4	0.73	12.6	0.69	14.6	0.64	17.6	0.56	20.3	0.52
7	7.3	0.89	8.8	0.85	10.6	0.80	12.7	0.74	15.6	0.67	18.6	0.60
8	7.5	0.72	8.7	0.73	10.3	0.72	12.4	0.69	15.6	0.60	18.4	0.55
9	10.5	0.80	11.2	0.81	12.3	0.80	12.7	0.79	14.6	0.75	16.1	0.73
10	9.8	0.82	10.8	0.82	11.8	0.83	12.3	0.79	13.7	0.77	15.3	0.76
11	9.2	0.85	10.3	0.83	11.1	0.81	12.5	0.77	14.3	0.73	16.2	0.72
12	2.3	0.83	3.0	0.81	4.7	0.75	7.2	0.67	8.8	0.63	10.1	0.62
13	2.0	0.78	2.6	0.74	4.0	0.70	6.2	0.64	7.6	0.63	10.9	0.60
14	2.4	0.83	3.3	0.81	5.0	0.75	7.2	0.69	8.7	0.66	10.2	0.65
15	3.7	0.85	4.7	0.80	6.3	0.71	8.4	0.62	11.7	0.59	14.5	0.56
16	2.8	0.88	5.0	0.86	5.6	0.80	6.8	0.77	5.9	0.77	5.2	0.74
17	3.4	0.81	4.3	0.80	6.4	0.71	9.0	0.64	11.3	0.62	13.5	0.60
18	7.0	0.89	7.7	0.87	8.6	0.85	10.3	0.82	12.1	0.80	14.0	0.77
19	7.4	0.92	8.5	0.89	9.3	0.84	11.0	0.79	13.2	0.76	15.8	0.71
20	7.4	0.69	6.8	0.49	7.7	0.48	9.1	0.47	12.7	0.57	15.7	0.45
21	7.0	0.61	7.9	0.62	9.0	0.72	10.8	0.72	12.7	0.70	14.8	0.65
22	2.1	0.82	3.2	0.77	4.4	0.72	6.3	0.67	7.4	0.66	8.2	0.70

where $T_{max,\,m}$ and $T_{min,\,m}$ are the maximum and minimum monthly ambient temperatures, respectively; and R is the ratio of amplitudes of ground to surface temperatures given by

$$R = 0.4 + 0.01\left(T_{amb,annual} - T_{ref}\right)1.8^{o}C^{-1} \tag{12}$$

where T_{ref} is a reference temperature assumed to be $21^{o}C$.

Finally, frequency (f_{annual}) and phase angles (α_{amb}, α_{mains}) in Eq. (9) are obtained assuming that the maximum temperature takes place on January 15th, thus

$$f_{annual} = \frac{1}{24}\frac{\alpha_{amb}}{\text{Dayofmax.temp.}} - 90^{o} \tag{13}$$

where $\alpha_{amb} = 104.8^{o}$ and α_{mains} is given as function of the ambient temperature as follows

$$\alpha_{mains} = 35^{o} - 0.01^{o}\left(T_{amb,annual} - T_{ref}\right)1.8^{o}C^{-1} \tag{14}$$

2.3. Estimation of the number of free-cooling hours

To evaluate the free-cooling availability, the study considers 8760 h of operation per year. The number of hours in which each of the operating modes is available (conventional, partial free-cooling and complete free-cooling) depends on the temperature leaving the economizer (state 27), which changes with the geographical location since the cooling tower interacts directly with the environment. An energy balance is conducted to calculate the thermodynamic state leaving the economizer, as follows

$$h_{27} = h_{26} - \frac{\varepsilon\dot{C}_{\min}\Delta T_{\max}}{\dot{m}_{27}} \tag{15}$$

which is assumed to be at the saturated liquid state. In Eq. (15), the minimum heat capacity rate is given by $\min(\dot{C}_{24}, \dot{C}_{26})$, whereas $\Delta T_{\max}$ requires an energy balance in the CWP.

The hourly variation of the environmental properties is estimated using the time at which the minimum and maximum take place and a curve fitting to a sinusoidal function, as suggested in [54]. Thus, the thermodynamic performance of the refrigeration system is evaluated for each hour of the year, allowing to estimate the availability of each of the operating modes, as well as the variations in COP and WER. Table 4 shows the monthly average temperature and RH at each of the selected stations.

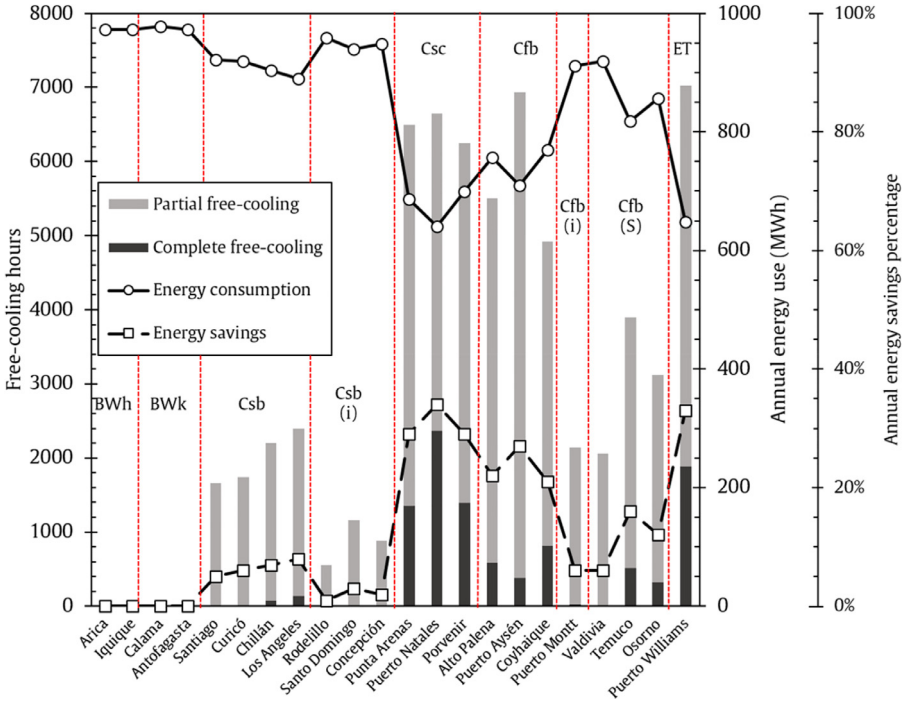

Fig. 3. Annual free-cooling availability and energy reduction opportunities.

3. Climatic influence upon system and component performances

This section intends to elucidate the effect of climate conditions on the thermodynamic performance of the system. Fig. 3 shows the available free-cooling hours per year at each of the selected locations. In desert climates (BWh and BWk) the economization is impossible. A similar behavior is observed in warm-summer Mediterranean climates (Csb), with less than 26% of partial free-cooling availability, for which the coastal influence (Csb (i)) reduces the partial economization to less than 13%.

The free-cooling availability turns significant in cool-summer Mediterranean with winter rain (Csc) and tundra climates (ET), offering a high number of both complete and partial free-cooling hours. This is explained by the low temperatures found in these climates, with an average annual temperature below 6.8°C (Table 4). Temperate climates (Cfb) also offer complete free-cooling hours, with an average annual temperature below 8°C, but the

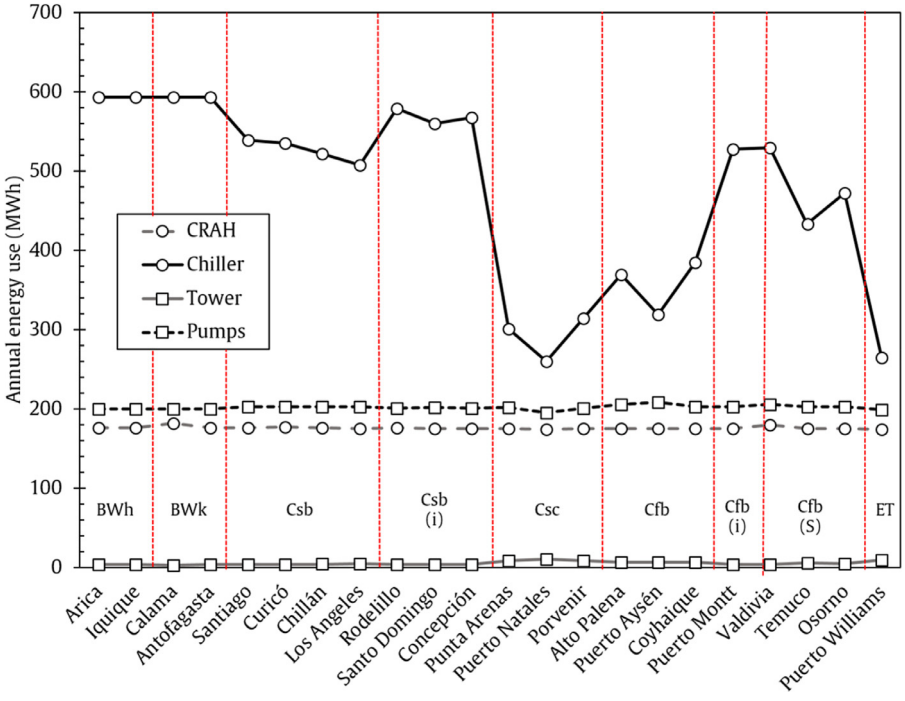

Fig. 4. Effect of climate conditions on the annual cooling energy use distribution.

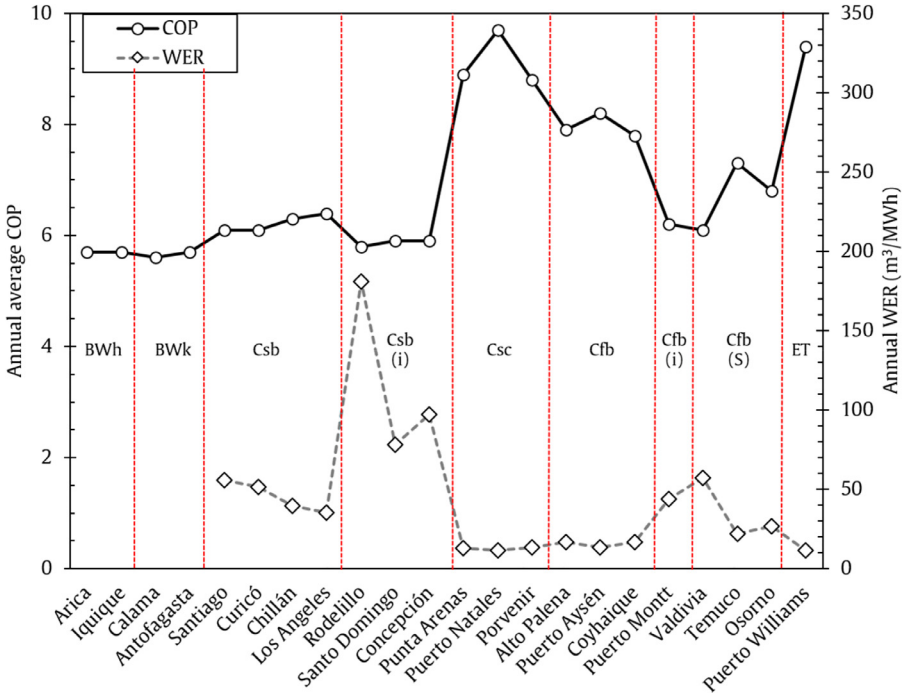

Fig. 5. Coefficient of performance and water required to achieve it.

Table 5
Percentage of the monthly availability of complete free-cooling.

Station	Jan	Feb	Mar	Apr	May	Jun	Jul	Aug	Sep	Oct	Nov	Dec
1	–	–	–	–	–	–	–	–	–	–	–	–
2	–	–	–	–	–	–	–	–	–	–	–	–
3	–	–	–	–	–	–	–	–	–	–	–	–
4	–	–	–	–	–	–	–	–	–	–	–	–
5	–	–	–	–	–	1.3	2.8	–	–	–	–	–
6	–	–	–	–	–	0.4	1.9	–	–	–	–	–
7	–	–	–	0.3	0.8	0.3	6.9	1.6	–	–	–	–
8	–	–	–	–	2.2	1.7	10.1	3.9	–	–	–	–
9	–	–	–	–	–	–	–	–	–	–	–	–
10	–	–	–	–	–	–	0.1	–	–	–	–	–
11	–	–	–	–	–	–	–	–	–	–	–	–
12	–	–	–	3.2	13.6	47.1	52.0	38.8	21.5	6.2	1.4	0.3
13	0.7	–	1.5	17.9	50.1	60.3	66.0	56.6	42.6	17.3	7.9	0.4
14	–	–	–	0.3	17.7	47.8	49.2	39.0	25.4	8.9	1.4	0.7
15	–	–	–	2.2	1.7	16.7	23.0	21.1	10.3	5.0	–	–
16	–	–	–	–	–	5.7	32.7	2.4	1.0	0.9	0.7	8.3
17	–	–	–	0.6	4.2	21.3	33.2	27.6	16.4	6.7	–	–
18	–	–	–	–	–	1.1	1.2	1.6	–	–	–	–
19	–	–	–	–	–	0.8	–	–	1.7	–	–	–
20	–	–	–	–	1.2	2.4	7.1	21.8	20.8	13.6	2.4	0.3
21	–	–	–	–	1.3	13.5	17.7	10.3	1.3	–	–	–
22	–	0.3	–	5.7	26.1	57.1	59.5	43.8	36.0	18.8	8.3	0.8

partial free-cooling is more important. Here, the coastal influence (Cfb (i)) reduces the partial free-cooling availability considerably to less than 24%.

Fig. 4 intends to elucidate which components are the most affected by variations in the climate conditions by showcasing their annual energy use distribution. The chiller energy use considerably decreases as the economizer availability increases, proving to be the component most affected by climate conditions. On the other hand, CRAH units, pumps and cooling tower show a fairly constant energy use distribution regardless of climate conditions, since their thermal performance remains unaffected by the environmental properties. Therefore, the overall energy use levels greatly depend on the chiller load.

Fig. 5 shows the annual energy required to dissipate the heat in excess from the racks, as well as the annual water supply required to achieve energy savings when economization is possible. The idea is to elucidate if the reductions in the cooling energy use due to the economizers lead to a significant increase in the water consumption. Here, both high COP and low WER values are desired. The results show that free-cooling is unavailable in desert climates; therefore, the lowest COP values are found (5.6–5.7). The highest water requirements are found in climates with coastal influence such as warm-summer Mediterranean with winter rain (Csb (i)). Considering that the COP is also low under these climates, water-side economization underperforms under these conditions. Warm-summer Mediterranean with winter rain (Csb), temperate rainy with coastal influence (Cfb (i)), and temperate rainy with short summer drought periods (Cfb (s)) climates all show a similar behavior; this is, a moderate increase in the COP (6.1–7.3) and relatively low WER values

Table 6
Percentage of the monthly availability of partial free-cooling.

Station	Jan	Feb	Mar	Apr	May	Jun	Jul	Aug	Sep	Oct	Nov	Dec
1	–	–	–	–	–	–	–	–	–	–	–	–
2	–	–	–	–	–	–	–	–	–	–	–	–
3	–	–	–	–	–	–	–	–	–	–	–	–
4	–	–	–	–	–	–	–	–	–	–	–	–
5	–	–	–	9.9	30.4	50.6	50.8	34.9	22.4	15.1	5.8	–
6	–	–	–	8.5	28.6	49.4	52.8	46.6	29.9	16.0	2.6	–
7	–	–	16.8	41.5	27.3	43.6	48.1	43.3	34.4	23.9	10.7	0.4
8	–	–	2.7	21.0	38.6	52.9	55.9	50.7	39.3	31.9	13.6	1.2
9	–	–	–	0.6	0.7	13.2	28.0	20.2	7.1	5.9	0.6	–
10	–	–	4.3	16.0	10.2	25.8	37.0	28.4	14.0	14.2	7.6	0.4
11	–	–	–	2.8	6.6	15.3	32.1	21.4	20.7	12.5	8.3	0.3
12	36.0	40.0	46.0	78.6	86.0	52.9	47.3	60.1	78.1	74.1	59.0	45.8
13	31.2	32.7	46.2	74.9	49.7	38.3	32.3	40.5	56.8	76.2	70.8	37.1
14	29.7	34.8	41.0	70.6	81.3	50.7	49.9	60.8	72.9	69.2	59.4	43.1
15	23.7	32.4	48.7	58.5	87.2	82.4	76.3	74.9	74.9	57.8	37.9	17.6
16	9.0	10.3	78.9	88.2	87.2	94.3	67.3	95.4	95.4	82.0	95.0	90.1
17	8.3	15.0	32.9	52.8	71.1	75.4	63.3	70.3	63.2	48.3	39.7	20.8
18	0.5	1.5	7.7	11.4	14.0	55.0	62.5	50.0	44.3	27.8	11.4	1.6
19	1.1	0.6	13.0	14.2	8.7	44.0	53.9	39.5	40.3	35.6	21.3	6.6
20	10.2	13.4	24.1	35.6	37.8	60.4	68.5	67.9	49.9	43.3	31.5	19.6
21	3.2	4.0	15.2	23.5	45.0	61.3	60.8	56.6	49.0	34.8	19.6	8.9
22	44.6	50.1	59.1	84.0	73.0	41.3	38.4	55.5	62.4	68.3	65.7	62.2

Table 7
Monthly COP variation.

Station	Jan	Feb	Mar	Apr	May	Jun	Jul	Aug	Sep	Oct	Nov	Dec
1	5.68	5.68	5.68	5.68	5.68	5.68	5.68	5.68	5.68	5.68	5.68	5.68
2	5.68	5.68	5.68	5.68	5.68	5.68	5.68	5.68	5.68	5.68	5.68	5.68
3	5.64	5.64	5.64	5.64	5.65	5.63	5.65	5.65	5.65	5.65	5.65	5.64
4	5.67	5.67	5.67	5.68	5.68	5.68	5.68	5.68	5.68	5.68	5.68	5.68
5	5.67	5.67	5.67	5.84	6.27	7.13	7.33	6.38	6.03	5.91	5.75	5.67
6	5.67	5.67	5.67	5.80	6.18	7.00	7.30	6.76	6.19	5.93	5.70	5.67
7	5.68	5.68	5.92	6.60	6.30	6.67	7.53	6.84	6.43	6.11	5.83	5.68
8	5.68	5.68	5.71	6.08	6.73	7.24	8.19	7.36	6.66	6.32	5.91	5.69
9	5.67	5.67	5.67	5.68	5.68	5.85	6.18	5.97	5.78	5.76	5.68	5.68
10	5.68	5.68	5.74	5.93	5.86	6.15	6.55	6.21	5.93	5.94	5.80	5.68
11	5.68	5.68	5.68	5.72	5.78	5.94	6.41	6.08	6.07	5.90	5.80	5.68
12	6.43	6.52	6.66	8.01	9.69	12.17	12.47	11.50	10.17	8.33	7.42	6.85
13	6.49	6.48	6.92	9.59	12.19	12.82	13.16	12.46	11.60	9.52	8.39	6.73
14	6.24	6.39	6.53	7.48	9.87	11.99	12.21	11.41	10.21	8.35	7.40	6.80
15	6.11	6.30	6.84	7.38	8.17	9.84	10.37	9.90	8.92	7.83	6.58	5.99
16	5.81	5.82	7.44	7.90	7.89	9.24	11.26	8.70	8.49	7.89	8.46	9.33
17	5.80	5.93	6.34	7.01	7.86	9.96	10.72	10.38	9.09	7.71	6.66	6.09
18	5.68	5.70	5.81	5.86	5.89	6.91	7.19	6.91	6.61	6.21	5.83	5.70
19	5.66	5.66	5.87	5.85	5.81	6.53	6.78	6.46	6.63	6.36	6.02	5.75
20	5.85	5.91	6.16	6.43	6.55	7.42	8.12	9.99	9.38	8.46	6.73	6.23
21	5.72	5.73	5.98	6.11	7.00	8.79	9.16	8.26	6.92	6.43	6.04	5.81
22	6.64	6.85	7.05	8.42	10.42	12.65	12.72	11.75	11.05	9.43	8.32	7.43

(22–57 m^3/MWh). The best opportunities for reductions in both cooling energy and water consumption are found in Cool-summer Mediterranean with winter rain (Csc), temperate rainy (Cfb) and tundra (ET) climates, in which the free-cooling availability is higher. Here the COP and WER range 7.8–9.7 and 11–17 m^3/MWh, respectively.

Since the four seasons are well defined in most of the Chilean territory, divided according to the astronomical timing for the southern hemisphere, a monthly analysis is presented to evaluate the system performance through the year. The following analysis and comments consider the average values among stations with identical climate conditions.

Table 5 shows the percentage of complete free-cooling hours per month at the selected locations. High complete free-cooling availability (>10%) is found in cool-summer Mediterranean with winter rain (Csc) and tundra (ET) climates from May to October (middle of fall to middle of spring). During winter time, the temperate rainy (Cfb) climate also shows complete free-cooling availability, which is reduced when short summer drought periods are present (Cfb (s)). None or negligible complete free-cooling availability is observed in all the remaining climates. In those climates, except in desert ones, the partial free-cooling appears as a potential solution for reducing the chiller load (Table 6).

In climates with available hours for complete economization (Cool-summer Mediterranean with winter rain, Tundra and Temperate rainy), Table 7 shows that the COP can achieve an important augmentation compared to the conventional operation without the economizer (~50 to 120% increase). Moreover, Table 8 indicates that the water consumption associated to the energy savings achieves the lowest values through the year (WER = 7–14 m^3/MWh).

In the remaining climates, in which partial economization is possible, the COP increases from ~10 to 45% (Table 7). For warm-summer Mediterranean with winter rain climates (Csb), the benefits of partial economization are only significant from the middle of fall to winter time (>10% increase in the COP); which

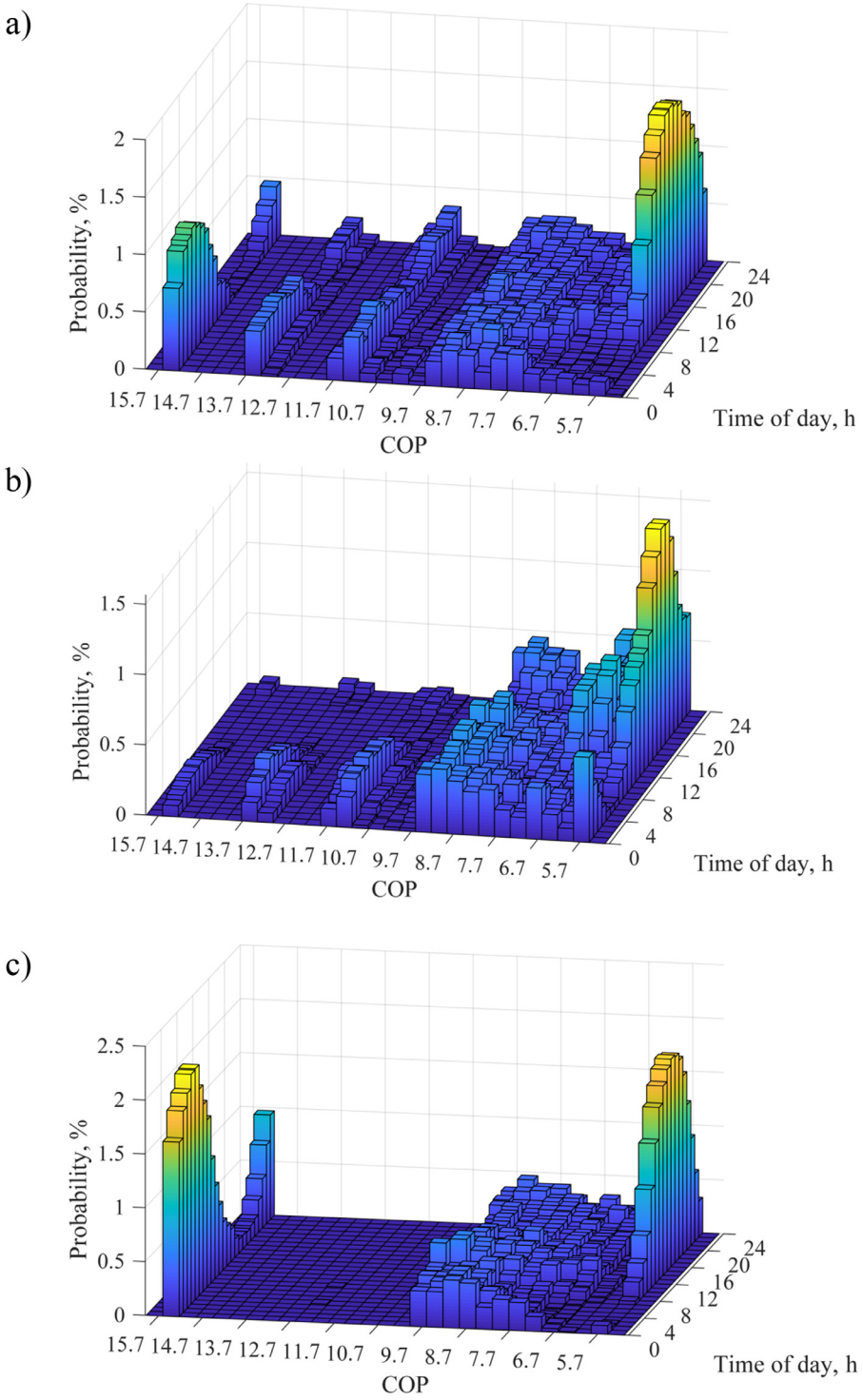

Fig. 6. Probability histogram of COP and time of day for (a) Csc, (b) Cfb and (c) ET.

is extended to late spring in temperate rainy with short summer drought periods climates (Cfb (s)).

In climates with coastal influence a COP increase above 10% is only possible during winter time. Table 7 and 8 show that climates with coastal influence, such as Csb (i) and Cfb (i), show a lower availability for economization, as well as low COP and high WER values, compared to Warm-summer Mediterranean with winter rain (Csb) and Temperate rainy (Cfb) climates, respectively. When compared to a climate with short summer drought periods (Cfb (s)), the coastal influence (Cfb (i)) also appears to diminish the system performance in terms of both cooling energy and water consumption.

Finally, Fig. 6 shows a bivariate probability histogram of COP as a function of the hours of the day. The results are shown for the climates that allow a significant number of hours of complete economization during the year (i.e., Cool-summer Mediterranean with winter rain (Csc), Temperate rainy (Cfb) and Tundra (ET)) and they are obtained by averaging the data of the locations with the same climate conditions. Each bar shows the probability of achieving a specific COP value at a specific time during the day, for

Table 8
Monthly WER variation (in m^3/MWh).

Station	Jan	Feb	Mar	Apr	May	Jun	Jul	Aug	Sep	Oct	Nov	Dec
1	–	–	–	–	–	–	–	–	–	–	–	–
2	–	–	–	–	–	–	–	–	–	–	–	–
3	–	–	–	–	–	–	–	–	–	–	–	–
4	–	–	–	–	–	–	–	–	–	–	–	–
5	–	–	–	120	41	20	19	36	62	89	229	–
6	–	–	–	146	46	22	20	26	46	83	523	–
7	–	–	79	28	37	25	18	23	31	49	112	1366
8	–	–	399	54	28	20	15	19	27	37	87	781
9	–	–	–	1286	1167	107	46	68	171	201	1285	–
10	–	–	269	76	103	46	28	41	77	76	148	2000
11	–	–	–	362	161	75	32	53	53	87	142	2541
12	35	32	28	15	10	8	8	8	10	14	19	25
13	34	34	24	11	8	8	8	8	9	12	15	28
14	43	36	31	17	10	8	8	9	10	15	19	26
15	57	43	25	19	14	10	9	10	12	17	31	73
16	145	132	17	14	14	10	8	11	12	15	12	10
17	159	83	38	22	16	10	8	10	13	18	29	58
18	1668	726	136	101	89	22	19	23	27	42	116	726
19	982	1254	102	106	136	35	28	37	33	40	67	200
20	114	87	47	33	32	19	15	12	13	16	29	49
21	397	309	69	50	23	14	13	15	23	33	60	142
22	28	24	21	13	9	8	7	8	9	12	15	18

which the sum of all bar heights is equal to one. All three climates show a high probability of achieving low COP values during the day, in which the system operates close to the conventional mode. It is during the early morning when the probability of reducing the energy use increases and the COP can achieve its highest values. This also occurs at the end of the day in Tundra (ET) climates.

4. Conclusions

The potential for implementing water-side economizers in the cooling system of data centers was investigated under different climate conditions by estimating the number of free-cooling hours available throughout the year. Chile was selected as case study due to the wide range of climate conditions found along the territory. A thermodynamics analysis aimed to investigate the opportunities of partially reducing the chiller load when complete economization is insufficient. For that, the system cooling energy and makeup water requirements were simultaneously evaluated and contrasted.

Due to their higher economization availability, Cool-summer Mediterranean with winter rain (Csc), temperate rainy (Cfb) and tundra (ET) climates offer higher COP and lower WER values. Most of the economization opportunities appear early in the morning during winter time. Throughout the year both Csc and ET climates offer a considerable number of partial free-cooling hours.

In desert climates the water-side economization is unfeasible. Warm-summer Mediterranean with winter rain (Csb) climates offer less than 26% of partial economization during the year, which is reduced to 13% when influenced by the coast (Csb (i)). Csc and ET climates both offer high availability of complete and partial free-cooling. In Cfb climates the number of free-cooling hours is also high; however, partial economization appears as the main mechanism for reducing the chiller load.

In terms of annual energy and water consumption, climates with coastal influence are not recommended for water-side economization. Such cases presented low COP and high WER values.

In general, in climates with lower availability of complete economization, the partial free-cooling offers good opportunities for reducing the cooling energy use, in particular during winter time. Even though the COP can be increased over 10% during winter time in climates with coastal influence, lower COP and higher WER values are found compared to climates without coastal influence and climates with short summer drought periods.

Declaration of Competing Interest

None.

Acknowledgment

This work was partially sponsored by CONICYT-Chile under project FONDECYT 11160172.

References

[1] J. Koomey, Growth in Data Center Electricity Use 2005 to 2010, Growth in Data Center Electricity Use 2005 to 2010, 9, Analytical Press, 2011 completed at the request of The New York Times.
[2] A. Shehabi, United States Data Center Energy Usage Report, Lawrence Berkeley National Laboratory, Berkeley, et al., California (2016) LBNL–1005775.
[3] The Green Grid, Guidelines for energy-efficient datacenters, The Green Grid, 2007 White Paper.
[4] M.A. Islam, et al., Water-constrained geographic load balancing in data centers, IEEE Trans. Cloud Comput. 5 (2) (2017) 208–220.
[5] D. Azevedo, S.C. Belady, J. Pouchet, Water Usage Effectiveness (WUE™): A Green Grid Datacenter Sustainability Metric (2011).
[6] B. Ristic, K. Madani, Z. Makuch, The water footprint of data centers, Sustainability 7 (8) (2015) 11260–11284.
[7] T. Gao, et al., Experimental and numerical dynamic investigation of an energy efficient liquid cooled chiller-less data center test facility, Energy Build. 91 (2015) 83–96.
[8] A. Bhalerao, et al., Rapid prediction of exergy destruction in data centers due to airflow mixing, Numer. Heat Transf. Part A Appl. 70 (1) (2016) 48–63.
[9] A.J. Díaz, et al., Energy and exergy assessment in a perimeter cooled data center: the value of second law efficiency, Appl. Therm. Eng. (2017) 820–830.
[10] K. Fouladi, et al., Optimization of data center cooling efficiency using reduced order flow modeling within a flow network modeling approach, Appl. Therm. Eng. 124 (2017) 929–939.
[11] L. Silva-Llanca, et al., Determining wasted energy in the airside of a perimeter-cooled data center via direct computation of the exergy destruction, Appl. Energy 213 (2018) 235–246.
[12] L. Silva-Llanca, et al., Cooling effectiveness of a data center room under overhead airflow via entropy generation assessment in transient scenarios, Entropy 21 (1) (2019) 98.
[13] A. Capozzoli, G. Primiceri, Cooling systems in data centers: state of art and emerging technologies, Energy Procedia 83 (2015) 484–493.
[14] J. Ni, X. Bai, A review of air conditioning energy performance in data centers, Renew. Sustain. Energy Rev. 67 (2017) 625–640.
[15] H. Zhang, et al., Free cooling of data centers: a review, Renew. Sustain. Energy Rev. 35 (2014) 171–182.
[16] Y.Y. Lui, Waterside and airside economizers design considerations for data center facilities, ASHRAE Trans. 116 (1) (2010) 98–108.
[17] J. Stein, Waterside economizing in data centers: design and control considerations, ASHRAE Trans. 115 (2) (2009) 192–200..
[18] E. Oró, et al., Energy efficiency and renewable energy integration in data centres. Strategies and modelling review, Renew. Sustain. Energy Rev. 42 (2015) 429–445.

[19] H.M. Daraghmeh, C.-.C. Wang, A review of current status of free cooling in datacenters, Appl. Therm. Eng. 114 (2017) 1224–1239.
[20] A.H. Khalaj, S.K. Halgamuge, A review on efficient thermal management of air-and liquid-cooled data centers: from chip to the cooling system, Appl. Energy 205 (2017) 1165–1188.
[21] L. Ling, Q. Zhang, L. Zeng, Performance and energy efficiency analysis of data center cooling plant by using lake water source, Procedia Eng. 205 (2017) 3096–3103.
[22] J. Wang, et al., Reliability and availability analysis of a hybrid cooling system with water-side economizer in data center, Build. Environ. 148 (2019) 405–416.
[23] M. Deymi-Dashtebayaz, S.V. Namanlo, A. Arabkoohsar, Simultaneous use of air-side and water-side economizers with the air source heat pump in a data center for cooling and heating production, Appl. Therm. Eng. 161 (2019) 114133.
[24] H. Cheung, S. Wang, Optimal design of data center cooling systems concerning multi-chiller system configuration and component selection for energy-efficient operation and maximized free-cooling, Renew. Energy (2019) 1717–1731.
[25] J. Niemann, et al., Economizer modes of data center cooling systems, Schneider Electric Data Center Science Center, Whitepaper 160 (2011).
[26] K. Dong, et al., Research on free cooling of data centers by using indirect cooling of open cooling tower, Procedia Eng. 205 (2017) 2831–2838.
[27] Y. Zhang, Z. Wei, M. Zhang, Free cooling technologies for data centers: energy saving mechanism and applications, Energy Procedia 143 (2017) 410–415.
[28] H. Zhang, et al., A review on thermosyphon and its integrated system with vapor compression for free cooling of data centers, Renew. Sustain. Energy Rev. 81 (2018) 789–798.
[29] J. Choi, J. Jeon, Y. Kim, Cooling performance of a hybrid refrigeration system designed for telecommunication equipment rooms, Appl. Therm. Eng. 27 (11–12) (2007) 2026–2032.
[30] A. Agrawal, M. Khichar, S. Jain, Transient simulation of wet cooling strategies for a data center in worldwide climate zones, Energy Build. 127 (2016) 352–359.
[31] E. Oró, et al., Overview of direct air free cooling and thermal energy storage potential energy savings in data centres, Appl. Therm. Eng. 85 (2015) 100–110.
[32] S.-.W. Ham, et al., Energy saving potential of various air-side economizers in a modular data center, Appl. Energy 138 (2015) 258–275.
[33] B.A. Hellmer, Consumption analysis of telco and data center cooling and humidification options, ASHRAE Trans. 116 (1) (2010) 118–133.
[34] J. Dai, D. Das, M. Pecht, Prognostics-based risk mitigation for telecom equipment under free air cooling conditions, Appl. Energy 99 (2012) 423–429.
[35] A. Shehabi, et al., Data center design and location: consequences for electricity use and greenhouse-gas emissions, Build. Environ. 46 (5) (2011) 990–998.
[36] J. Cho, Y. Kim, Improving energy efficiency of dedicated cooling system and its contribution towards meeting an energy-optimized data center, Appl. Energy 165 (2016) 967–982.
[37] J. Cho, et al., Development of an energy evaluation and design tool for dedicated cooling systems of data centers: sensing data center cooling energy efficiency, Energy Build. 96 (2015) 357–372.
[38] L. Phan, C.-.X. Lin, A multi-zone building energy simulation of a data center model with hot and cold aisles, Energy Build. 77 (2014) 364–376.
[39] H. Bulut, M.A. Aktacir, Determination of free cooling potential: a case study for Istanbul, Turkey, Appl. Energy 88 (3) (2011) 680–689.
[40] J. Siriwardana, S. Jayasekara, S.K. Halgamuge, Potential of air-side economizers for data center cooling: a case study for key Australian cities, Appl. Energy 104 (2013) 207–219.
[41] V. Depoorter, E. Oró, J. Salom, The location as an energy efficiency and renewable energy supply measure for data centres in Europe, Appl. Energy 140 (2015) 338–349.
[42] K.-.P. Lee, H.-.L. Chen, Analysis of energy saving potential of air-side free cooling for data centers in worldwide climate zones, Energy Build. 64 (2013) 103–112.
[43] J. Cho, T. Lim, B.S. Kim, Viability of datacenter cooling systems for energy efficiency in temperate or subtropical regions: case study, Energy Build. 55 (2012) 189–197.
[44] S.-.W. Ham, J.-.W. Jeong, Impact of aisle containment on energy performance of a data center when using an integrated water-side economizer, Appl. Therm. Eng. 105 (2016) 372–384.
[45] J.-.Y. Kim, et al., Energy conservation effects of a multi-stage outdoor air enabled cooling system in a data center, Energy Build. 138 (2017) 257–270.
[46] H. Tian, Z. He, Z. Li, A combined cooling solution for high heat density data centers using multi-stage heat pipe loops, Energy Build. 94 (2015) 177–188.
[47] B. Durand-Estebe, et al., Simulation of a temperature adaptive control strategy for an IWSE economizer in a data center, Appl. Energy 134 (2014) 45–56.
[48] A.H. Khalaj, T. Scherer, S.K. Halgamuge, Energy, environmental and economical saving potential of data centers with various economizers across Australia, Appl. Energy 183 (2016) 1528–1549.
[49] S. Klein, F. Alvarado, Engineering Equation Solver Software (EES), F-Chart Software, Madison, WI, USA, 2013.
[50] J.M. Cardemil, A.K. da Silva, Parametrized overview of CO2 power cycles for different operation conditions and configurations–an absolute and relative performance analysis, Appl. Therm. Eng. 100 (2016) 146–154.
[51] E.W. Lemmon, M.O. McLinden, M.L. Huber, M.O. McLinden, NIST reference fluid thermodynamic and transport properties–REFPROP, Version 7.0, NIST Standard Reference Database 23 (2002).
[52] M.E. Meakins, Energy and Exergy Analysis of Data Center Economizer systems, in Mechanical and Aerospace Engineering, San Jose State University, 2011.
[53] P. GŐsi, Method and chart for the determination of evaporation loss of wet cooling towers, Heat Transf. Eng. 10 (4) (1989) 44–49.
[54] J. Burch, C. Christensen, Towards development of an algorithm for mains water temperature, in: Proceedings of the Solar Conference, Citeseer, 2007.